DOI: 10.1002/chem.200901884

Hydroxypyridinechromene and Pyridinechalcone: Two Coupled Photochromic Systems

Yoann Leydet, A. Jorge Parola,* and Fernando Pina*[a]

Abstract: Substitution of the phenyl group in 2-hydroxychalcones by a 4-pyridine unit dramatically changes the network of chemical reactions of this compound: *trans*-chalcone-type (**Ct**), *cis*-chalcone-type (**Cc**), and a hemiketal (hydroxy-4-pyridinechromene) (**B**) and their protonated forms are formed, but the presence of a flavylium-type cation could not be detected even at very acidic pH values. Moreover, whereas in 2-phenyl-2-benzopyrylium compounds **B** and **Cc** are generally elusive species whose kinetic processes in aqueous solutions occur on the sub-second timescale, in the present compound these species equilibrate on a timescale four orders of magnitude lower. Complete characterization of the equilibrium and kinetics of the reaction network could thus be achieved by ^{1}H NMR spectroscopy and UV/Vis spectrophotometry. The network of chemical reactions exhibits *cis–trans* photoisomerization, as well as photochromism between the hemiketal and the chalcone-type species. The irradiation of **Ct** in MeOH/H_2O (1:1) at 365 nm produces **B** almost quantitatively through two consecutive photochemical reactions: **Ct**→**Cc** photoisomerization followed by **Cc**→**B** photo ring closure with a global quantum yield of 0.02. On the other hand, irradiation of **B** at 254 nm leads to a photostationary state composed by 80% **Ct** and 20% **B**, with a quantum yield of 0.21.

Keywords: chromenes · isomerization · multistate systems · photochromism · tautomerism

Introduction

Chromenes constitute one of the major classes of naturally occurring compounds and prove to be particularly attractive in medical sciences[1] as well as in chemistry due to their particular photochromism based on electrocyclic ring-opening at the pyran C–O bond.[2] The photochromism of chromenes was extensively studied and the mechanism established by Becker and co-workers.[3] These authors showed that these molecules, upon UV irradiation, yield open metastable photoproduct(s) with the structure of *o*-quinone allides, which are generally colored due to increased electronic delocalization. The photoproducts can recover thermally and/or photochemically to the starting material. This family of photochromic compounds, which covers a variety of structures such as benzo- and naphthopyrans bearing alkyl, oxoalkyl, or aromatic substituents, spiropyrans, and spirooxazines, is able to perform coloration/decoloration cycles with an efficiency close to unity and with a strong resistance to photodegradation.[2] Kinetics of coloration and/or decoloration can be also tuned through choice of substituents, which allows one to envisage the use of chromenes for many applications such as the development of optical variable transmission materials and optical switches and memories.[4]

It is worth noting that chromenes appear in the network of chemical reactions taking place in 2-phenyl-1-benzopyrylium derivatives (flavylium salts) that possess the same basic structure of anthocyanins, the ubiquitous colorants responsible for most of the red and blue colors of flowers and fruits.[5] In particular, hydroxyphenylchromenes appear as transient hemiketal species during the thermal conversion (pH jump) between flavylium cations and *trans*-chalcones as well as during the appearance of the flavylium cation/quinoidal base upon irradiation of *trans*-chalcone (Scheme 1).[6,7]

The network of chemical reactions occurring in flavylium compounds is shown in Scheme 1. The equilibrium species at sufficiently acidic pH values is the flavylium cation $\mathbf{AH}^+$. When the pH is raised, the flavylium cation undergoes hydration to give the hemiketal **B** (chromene). The *cis*-chal-

[a] Dr. Y. Leydet, Dr. A. J. Parola, Prof. F. Pina
Departamento de Química, REQUIMTE
Faculdade de Ciências e Tecnologia
Universidade Nova de Lisboa (Portugal)
Fax: (+35) 121-294-8550
E-mail: fjp@dq.fct.unl.pt
ajp@dq.fct.unl.pt

Supporting information for this article is available on the WWW under http://dx.doi.org/10.1002/chem.200901884.

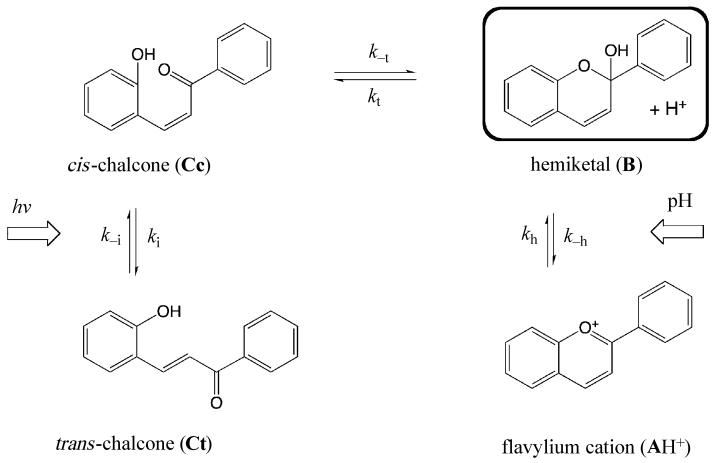

Scheme 1. Hydroxyphenylchromene (hemiketal, **B**) as part of the network of chemical reactions involving 2-phenyl-1-benzopyrylium compounds.

cone (**Cc**) is formed from **B** by a tautomeric ring-opening process and the *trans*-chalcone (**Ct**) by isomerization of the former. The system can proceed forward and backward by the action of the pH and light.[8]

The reactions occurring in Scheme 1 can be accounted for by means of the following set of equations [Eqs. (1), (2), and (3)]:

$$\mathbf{A}H^+ + 2\,H_2O \rightleftharpoons \mathbf{B} + H_3O^+ \quad K_h \tag{1}$$

$$\mathbf{B} \rightleftharpoons \mathbf{Cc} \quad K_t \tag{2}$$

$$\mathbf{Cc} \rightleftharpoons \mathbf{Ct} \quad K_i \tag{3}$$

Equations (1) to (3) can be substituted by a single acid–base equilibrium,[8] as shown by Equation (4):

$$\mathbf{A}H^+ + 2\,H_2O \rightleftharpoons \mathbf{CB} + H_3O^+ \quad K'_a \tag{4}$$

in which $[\mathbf{CB}] = [\mathbf{B}] + [\mathbf{Cc}] + [\mathbf{Ct}]$ and $K'_a = K_h + K_h K_t + K_h K_t K_i$.

According to the nature of the substituents in the flavylium backbone, the mole fraction distribution of the conjugated base **CB** can be constituted by 1) almost 100% of **Ct** when hydroxy[8] or amino[9] substituents are present in positions 7 and/or 4′; 2) a majority of **B** in 3-substituted flavylium compounds,[10] as in anthocyanins (ca. 68% in malvidin diglucoside),[11] or 3) exclusively **A** in the case of 4-methylflavylium compounds bearing hydroxyl substituents.[12]

In previous papers, the photochemistry of the *trans–cis* isomerization of 2-hydroxychalcones was extensively studied by our group[8,9,13] and other authors.[14–16] Irradiation of the *trans*-chalcone in pure aqueous solutions or in water/organic solvent mixtures leads to **Cc** and/or **B** that rapidly form a flavylium cation or quinoidal base depending on pH. In organic solvents, irradiation of the *trans*-chalcone (**Ct**) leads to **Cc** and/or **B**, as suggested by the groups of Czerney,[15] Matsushima,[14g] and Hiratsuka,[17] even if, with the exception of the last author, only scarce experimental evidence was given to prove the existence of **B** (or **Cc**) as photoproducts. On the other hand, irradiation of **Cc** or **B** could give back the **Ct** species. In aqueous media, the **B** and **Cc** species are generally in fast equilibrium, and it is not possible to exclude excitation of **Cc** while irradiating **B** due to the superposition of their absorption spectra. In other words, no strong evidence for the selective irradiation of the hemiketal **B** was reported in those works.

Taking into account the reaction network in Scheme 1, the introduction of positively charged groups in the 2-hydroxychalcone skeleton may avoid formation of the flavylium cation at acidic pH, thereby promoting the stability of the hemiketal/chromene species over a large pH range. Substitution of the phenyl attached to the carbonyl group of the chalcone by a pyridine could in principle lead to this desideratum.

In this paper, we report on the synthesis, thermodynamics, kinetics, and photochemistry of a new pyridinechalcone compound in which the phenyl group has been substituted by a 4-pyridine moiety. The reaction network of this compound includes **Ct**-, **Cc**-, and **B**-type compounds (and their protonated forms) and excludes formation of the flavylium-type cation, even at very acidic pH values.

Results and Discussion

Thermodynamic equilibrium: Compound **1** was synthesized by condensation of salicylaldehyde with 4-acetylpyridine under basic conditions (ethanol/KOH). The absorption spectra of a freshly prepared solution of **1** in MeOH/H_2O (1:1) upon pH jumps that cover the full pH range are represented in Figure 1. Figure 1A and B depict the spectra immediately after each pH jump, and Figure 1C and D are at the equilibrium.

The absorption spectra reported in Figure 1A and B show the existence of two different sets of isosbestic points, which can be attributed to the several acidic and basic species of **1**, hereafter designated as *trans*-chalcones $\mathbf{Ct}^+$, **Ct**, and $\mathbf{Ct}^-$, as shown in Scheme 2. The first set regards the protonation of the pyridine (Figure 1A, $pK_a^{\mathbf{Ct}^+} = 3.2$) and the second one the deprotonation of the phenol (Figure 1B, $pK_a^{\mathbf{Ct}} = 8.9$). The first pK_a value is comparable to 3.6 for 4-acetylpyridine,[18] and the second one is in accordance with the usually observed pK_a values in similar 2-hydroxychalcones, in which the pyridine is substituted for phenyl.[9b,19] Whereas the absorption spectra in the neutral and basic regions do not evolve significantly with time, as evidenced by comparing Figure 1B and D, in acidic media the solutions present completely different spectra over time, as shown in Figure 1A and C. This means that although **Ct** and $\mathbf{Ct}^-$ are the clearly predominant equilibrium species in the neutral and basic regions, in the acidic region $\mathbf{Ct}^+$ evolves to other species.

The spectral variations in the acidic region are not compatible with flavylium-type cation formation since the char-

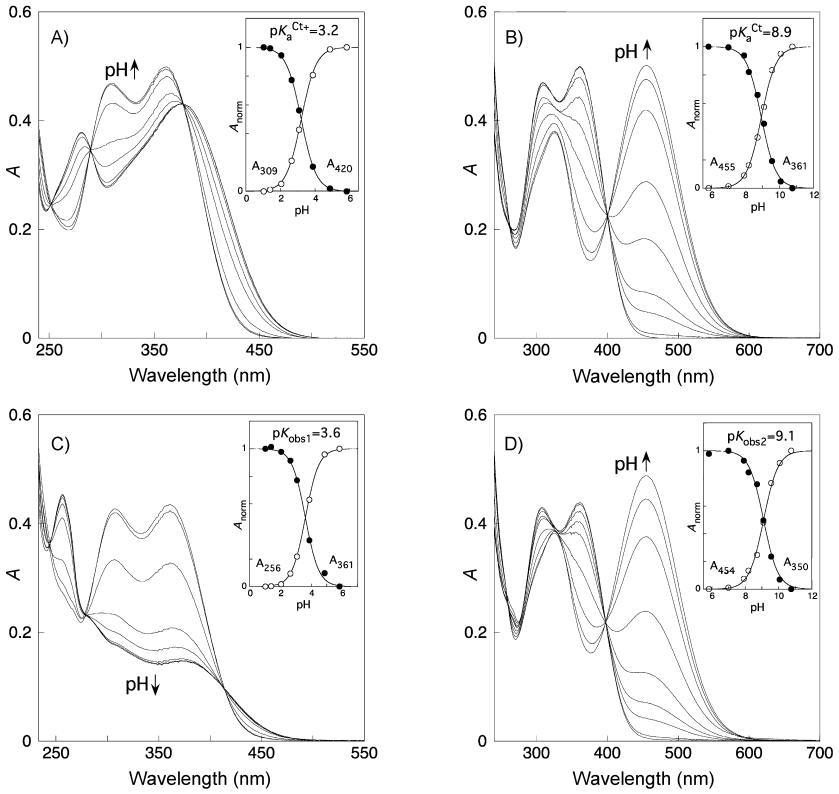

Figure 1. Absorption spectra of freshly prepared **1** in methanol/water (1:1) as a function of pH, immediately after pH jumps to the A) acidic and B) basic regions, and after thermal equilibration in the dark (2 d, (295 ± 1) K), C and D, acid and basic regions, respectively.

values of the systems by 2–3 pH units.[20,21] The kinetics of the disappearance of protonated *trans*-chalcone **Ct**$^+$ in an acidic medium is very slow and approximately 48 h are needed to reach a complete equilibration at room temperature ((295 ± 1) K), which is in agreement with the existence of a *cis–trans* isomerization barrier.[22]

To fully characterize the species involved in the network, ^{1}H NMR spectroscopic studies were performed at different pD values. Figure 2 shows the NMR spectra as a function of pD for freshly prepared solutions and for the same solutions upon thermal equilibration in the dark (full assignment of peaks is presented in Table S1 in the Supporting Information). The ^{1}H NMR spectrum of freshly prepared (CD_3OD/D_2O 1:1) neutral solution of compound **1** is shown in Figure 2c. The *trans*-chalcone **Ct** was unequivocally identified by the

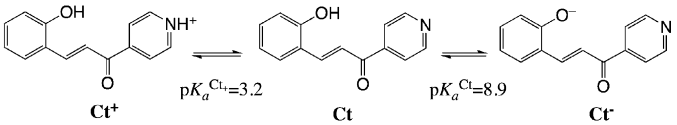

1

Scheme 2. Acid–base species of compound **1** and their respective pK_a values.

acteristic absorption band of **A**H$^+$, always redshifted relatively to **Ct**, is not observed in the visible region of the spectra. According to ^{1}H NMR spectroscopy (see below), the mole fraction distribution at the equilibrium at pH 0.3 is a mixture of **Ct**$^+$ (37%) and approximately equal amounts of protonated *cis*-chalcone (**Cc**$^+$) and hemiketal (**B**$^+$), approximately 31.5% of each one.

The lack of flavylium cation can be explained by the protonation of the pyridine at pH values where formation of the flavylium cation would be expected.[6–8] The positive charge in the pyridinium moiety prevents the formation of a 2+ charged species due to the intramolecular electrostatic repulsion. This result is in agreement with the behavior of 2-phenyl-1-benzopyrylium systems in cetyltrimethylammonium bromide (CTAB) micelles, in which the positively charged surface of the micelle renders the formation of the flavylium cation more difficult, thereby lowering the pK'_a

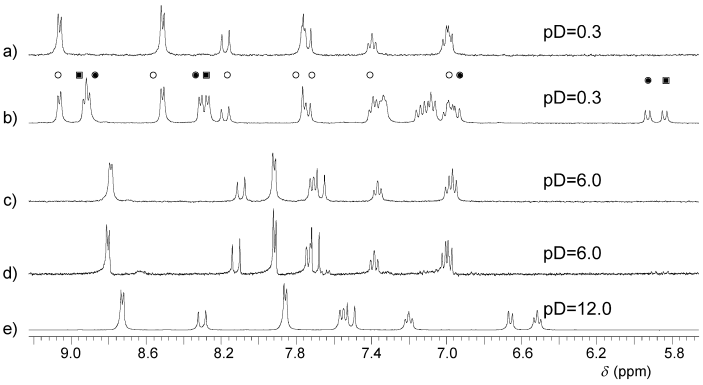

Figure 2. ^{1}H NMR spectra (400 MHz, 300 K) of **1** in D_2O/CD_3OD 1:1 at different pD values, immediately after dissolution (traces, a, c, and e) and upon thermal equilibration in the dark (traces b and d); **Ct**$^+$ (○); **B**$^+$ (●); **Cc**$^+$ (■).

coupling constant between protons H3 and H4 (^3J(H3,H4) = 16.0 Hz). Upon thermal equilibration (ca. 2 days at (295 ± 1) K), the spectrum in Figure 2d shows that two new species were formed in very low extension, most probably **Cc** and **B**. Dissolution of compound **1** under basic conditions (CD_3OD/D_2O 1:1, NaOD; pD = 12.0) leads to a high-field shift of the spectrum relative to the neutral solution (Figure 2e) with a concomitant change in color from light yellow

to orange. These changes indicate the formation of $\mathbf{Ct}^-$, confirmed also by the persistent large value of the coupling constant of the protons on the C=C double bond, $^3J(H3,H4) = 15.9$ Hz. The spectra of the $\mathbf{Ct}^-$ species evolves only slightly with time and apparently originates two new species in low extension (<5%; not shown).

When the neutral light yellow solution of freshly prepared **Ct** is subjected to a pD jump to pD = 0.3, the yellow coloration increases. The ^{1}H NMR spectrum registered immediately after addition of a drop of concentrated DCl (Figure 2a) shows the existence of a sole species with peaks shifted to low field, which is compatible with the formation of protonated *trans*-chalcone $\mathbf{Ct}^+$, as confirmed by the coupling constant around the C=C double bond ($^3J(H3,H4) = 15.8$ Hz; Table S1 in the Supporting Information). The large changes in the chemical shifts of the pyridine protons (Table S1) relative to the others are one piece of evidence for the protonation of the pyridine nitrogen. Contrary to what was observed under neutral and basic conditions, in acidic media the spectrum of $\mathbf{Ct}^+$ largely evolves in time with the appearance of two new species in almost equal amounts (Figure 2b) with a concomitant change in color to light yellow. These results are consistent with the formation of $\mathbf{Cc}^+$, followed by a tautomerization (ring opening) that leads to the protonated hemiketal (hydroxy-4-pyridinechromene) $\mathbf{B}^+$, as confirmed by ^{1}H and ^{13}C NMR spectroscopy (see below). No $\mathbf{A}H^+$ could be detected under acidic conditions, even at pH < −1 (concd H_2SO_4).

The spectra of thermally equilibrated solutions in the dark registered in the acidic region show three sets of peaks corresponding to $\mathbf{B}/\mathbf{B}^+$, $\mathbf{Cc}/\mathbf{Cc}^+$, and $\mathbf{Ct}/\mathbf{Ct}^+$ (the acid–base pairs are in fast equilibrium on the NMR spectroscopic timescale), as can be seen in the traces of Figure 2b and d. Experiments run at several intermediate pH values (Figure S1 in the Supporting Information) corroborate these data and allow one to obtain the distribution of the three acid–base conjugate pairs present in equilibrated solutions in the acidic pH region (Figure 3).

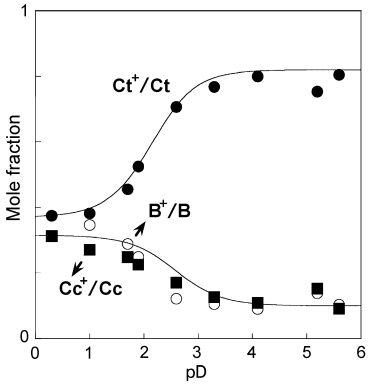

Figure 3. Distribution of the species constituting the reaction network of compound **1** in the acidic region according to ^{1}H NMR spectroscopic data in Figure 2 (see also Figure S1 in the Supporting Information): normalized areas of the peaks corresponding to $\mathbf{Ct}^+/\mathbf{Ct}$ H3′5′ (●); $\mathbf{B}^+/\mathbf{B}$ H3 (○); $\mathbf{Cc}^+/\mathbf{Cc}$ H3 (■).

The NMR spectroscopic data in Figure 3 presents three plateaus between pD = 3.5 and pD = 6 that allow one to calculate $K_i = 8.0$ and $K_t = 1.0$. Similarly, for pD < 1, three other plateaus arise and yield $K_{i+} = 1.2$ and $K_{t+} = 1.0$. In combining these data with the two pK_a values of **Ct** obtained by UV/Vis spectrophotometry (Figure 1A and B), the following reaction network and respective equilibrium constants for the acid-neutral region can be drawn (Scheme 3).

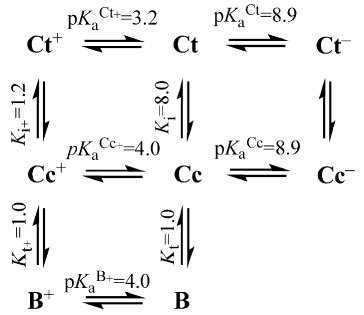

Scheme 3. Thermodynamic equilibria present in methanolic aqueous solutions (1:1) of compound **1**. The pK_a values for **Ct** were obtained from Figure 1A and B; $pK_a^{Cc^+}$ was obtained through $K_a^{Cc^+} = K_a^{Ct^+} K_{i+}/K_i$; $pK_a^{B^+}$ was obtained through $K_a^{B^+} = K_a^{Cc^+} K_{t+}/K_t$; the other equilibrium constants were obtained from the NMR spectroscopic data in Figure 3.

On the basis of Scheme 3, the total concentration of compound **1** is given by Equation (5):

$$C_0 = [\mathbf{Ct}^+]+[\mathbf{Cc}^+]+[\mathbf{B}^+]+[\mathbf{Ct}]+[\mathbf{Cc}]+[\mathbf{B}]+[\mathbf{Ct}^-]+[\mathbf{Cc}^-] \quad (5)$$

By using Equation (5), individual expressions for the mole fraction of each species can be obtained as a function of proton concentration and the equilibrium constants $K_a^{Ct^+}$, $K_a^{Cc^+}$, $K_a^{B^+}$, K_a^{Ct}, K_a^{Cc}, K_{i+}, and K_{t+} [Eqs. (S1)–(S9) in the Supporting Information].

The absorption spectra in Figure 1C and D present clear isosbestic points, which suggest that the overall system after equilibration behaves with pH as a diprotic species. In summing up the mole fractions of the corresponding protonated species, the expressions obtained are indeed compatible with this interpretation [Eqs. (6), (7), and (8)]:

$$\frac{[\mathbf{Ct}^+]+[\mathbf{Cc}^+]+[\mathbf{B}^+]}{C_0} = \frac{[H^+]^2}{[H^+]^2+K_{obs1}[H^+]+K_{obs1}K_{obs2}} \quad (6)$$

$$\frac{[\mathbf{Ct}]+[\mathbf{Cc}]+[\mathbf{B}]}{C_0} = \frac{K_{obs1}[H^+]^2}{[H^+]^2+K_{obs1}[H^+]+K_{obs1}K_{obs2}} \quad (7)$$

$$\frac{[\mathbf{Ct}^-]+[\mathbf{Cc}^-]}{C_0} = \frac{K_{obs1}K_{obs2}}{[H^+]^2+K_{obs1}[H^+]+K_{obs1}K_{obs2}} \quad (8)$$

with the following expressions for the observed acidity constants [Eqs. (9) and (10)]:

$$K_{obs1} = \frac{K_a^{B^+} + K_a^{Cc^+}K_{t+} + K_a^{Ct^+}K_{t+}K_{i+}}{1 + K_{t+} + K_{t+}K_{i+}} \quad (9)$$

$$K_{obs2} = \frac{K_a^{Cc}K_a^{Cc^+}K_{t+} + K_a^{Ct}K_a^{Ct^+}K_{t+}K_{i+}}{1 + K_{t+} + K_{t+}K_{i+}} \quad (10)$$

With the exception of the acidity constants related to $\mathbf{Cc}^+$, $\mathbf{B}^+$, and **Cc**, the thermodynamic constants intervening in Equations (9) and (10) are known either from UV/Vis ($K_a^{Ct^+}$) or ^{1}H NMR spectroscopy (K_{i+}, K_i, K_{t+}, K_t) experiments. The acidity constants $K_a^{Cc^+}$ and $K_a^{B^+}$ can be calculated from $K_a^{Cc^+} = K_a^{Ct^+}K_{i+}/K_i$ and $K_a^{B^+} = K_a^{Cc^+}K_{t+}/K_t$, respectively, and were included in Scheme 3. Assuming that K_a^{Cc} is similar to K_a^{Ct}, as often observed in 2-hydroxychalcones,[21] and substituting all constants in Equations (9) and (10), $pK_{obs1} = 3.5$ and $pK_{obs2} = 9.0$ are obtained, which is in good agreement with the values obtained experimentally in Figure 1C and D, respectively.

It is worth noting that the composition at equilibrium under acidic conditions in the reaction network of compound **1** can be tuned by changing the solvent. Whereas in a solvent mixture MeOH/H_2O 1:1 the distribution of species is the one represented in Figure 3, in pure acidic water only $\mathbf{Ct}^+$ and $\mathbf{B}^+$ (45:55) can be detected as shown by ^{1}H NMR spectroscopy (Figure S2 in the Supporting Information).

The absorption spectra of all the species present in methanolic aqueous solutions of compound **1** could be deduced by combining UV/Vis and ^{1}H NMR spectroscopic data (Figure 4). The spectrum of **Ct** is dominated by a typical chalcone transition in the near-UV region ($\lambda_{max} = 362$ nm). Both the protonation of the pyridine and the deprotonation of the phenol group lead to a redshift of λ_{max} in agreement with an increase of the charge delocalization in the structures of $\mathbf{Ct}^+$ and $\mathbf{Ct}^-$ ($\lambda_{max} = 383$ nm and $\lambda_{max} = 455$ nm, respectively). The spectrum of **B** was obtained upon irradiation of **Ct** at 365 nm until the stationary state was reached (it contains 100% **B**; see below), whereas that of **Cc** was obtained from the same solution after thermal equilibration and determining the composition by ^{1}H NMR spectroscopy (80% **Ct**+10% **B**+10% **Cc**). The two species are characterized by opposite maximum wavelength shifts relative to the **Ct** band maximum. Whereas **B** shows a strong blueshift ($\lambda_{max} = 296$ nm), the spectrum of **Cc** presents comparatively a slight redshift ($\lambda_{max} = 380$ nm).

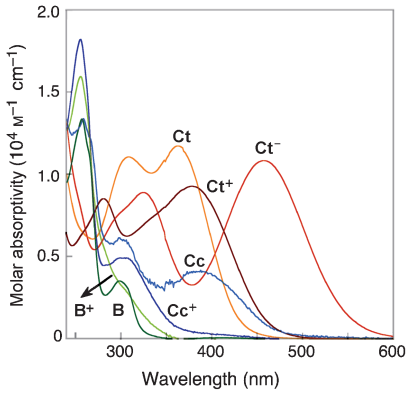

Figure 4. Absorption spectra of the several species originating from compound **1** in H_2O/CH_3OH 1:1: pH≈1 for $\mathbf{B}^+$ (H_2O), $\mathbf{Cc}^+$, and $\mathbf{Ct}^+$; pH≈6 for **B**, **Cc**, **Ct**; pH≈12 for $\mathbf{Ct}^-$. The spectra were obtained in the following way: **Ct**, $\mathbf{Ct}^-$, $\mathbf{Ct}^+$ came from Figure 2A and B; **B** was obtained from an irradiated solution of **Ct**; $\mathbf{B}^+$ was obtained upon thermal equilibration of **Ct** in water at pH 1.0 (45% $\mathbf{Ct}^+$+55% $\mathbf{B}^+$); $\mathbf{Cc}^+$ was obtained from equilibrated solution at pH≈1 (37% $\mathbf{Ct}^+$+31.5% $\mathbf{B}^+$+31.5% $\mathbf{Cc}^+$), assuming that the spectrum of $\mathbf{B}^+$ does not change significantly on going from H_2O to H_2O/CH_3OH 1:1; **Cc** was obtained from irradiated solutions of **Ct** upon thermal recovery (80% **Ct**+10% **B**+10% **Cc**).

Theoretical calculations using ZINDO-S/CI (99 single excited configurations) on AM1-RHF-optimized geometries confirmed the relative energies of the lowest-energy electronic transitions experimentally observed (Table S2 in the Supporting Information). In the case of the **B** species, the conjugation between the pyridine and the phenol ring is interrupted after formation of the hemiketal middle ring, thus explaining the observed blue shift. In the **Cc** species, three minimum energy conformers could be found, two of them with coplanarity of the conjugated system and a zwitterionic and nonplanar conformer. In one of the planar conformers (Figure 5, left), an intramolecular hydrogen bond between the proton of the phenol and the oxygen of the carbonyl group is formed, and the predicted λ_{max} according to the molecular orbital calculations is redshifted relative to **Ct** (Table S2). The other planar conformer (not shown), in which the phenol ring is rotated 180° relative to that in Figure 5 (left), and the zwitterionic form (not shown) are predicted to have nearly the same λ_{max} as **Ct**. On this basis, the fact that the **Cc** λ_{max} is redshifted relative to that of **Ct** (Figure 4) suggests that **Cc** may have a significant amount of the hydrogen-bonded conformer in solution.

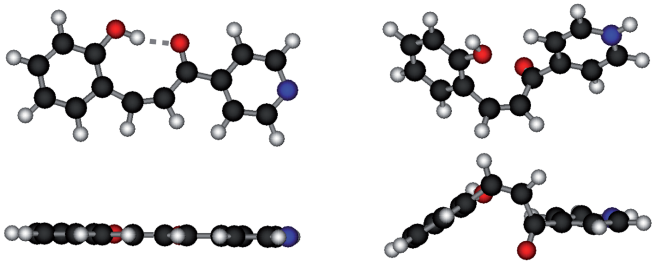

Figure 5. Minimum-energy conformers of **Cc** (left) and $\mathbf{Cc}^+$ (right) optimized using the AM1-RHF semiempirical method implemented in the Hyperchem 7.5 package.[30]

In MeOH/H_2O 1:1 solvent mixtures, $\mathbf{B}^+$ and $\mathbf{Cc}^+$ could not be isolated from each other due to the fast tautomerization process under acidic conditions. However, a spectrum of $\mathbf{B}^+$ was obtained in pure aqueous solution at pH 1.0 where no $\mathbf{Cc}^+$ is observed, as confirmed by ^{1}H NMR spectroscopy (Figure S2 in the Supporting Information). Assuming that the spectrum of $\mathbf{B}^+$ does not change significantly on going from acidic water to acidic methanolic aqueous solutions (in which $\mathbf{B}^+$ exists in equilibrium with $\mathbf{Cc}^+$; Figure 2b), the spectrum of $\mathbf{Cc}^+$ could be deduced. Contrary to

the $\mathbf{Ct}^+/\mathbf{Ct}$ pair in which $\mathbf{Ct}^+$ is redshifted relative to **Ct**, the λ_{max} of $\mathbf{Cc}^+$ (305 nm) is strongly blueshifted relative to **Cc**. Indeed, theoretical calculations showed that the protonation of the pyridine disrupts the intramolecular hydrogen bond in a conformation that is no longer planar (Figure 5, right). This interruption in the conjugation between the pyridine and the phenol rings is compatible with the observed blueshift (Table S2). The spectrum of $\mathbf{B}^+$ showed no significant shift after the protonation of pyridine in **B**, which is in agreement with the exclusion of the pyridine ring from conjugation as already observed with **B**.

Kinetic studies: Thermally equilibrated solutions of **Ct** at neutral pH in MeOH/H_2O 1:1 contain only a small proportion of **Cc** and **B** (see Figure 2d), thus rendering a kinetic study of the reaction difficult. However, irradiated solutions of **Ct** in the same conditions lead to approximately 100% **B** (see below), thereby allowing the thermal recovery kinetics study of the irradiated solutions.

To distinguish between **B** and **Cc**, the thermal evolution after irradiation was followed by ^{1}H NMR spectroscopy at four different temperatures. As an example, the results for $T = 308$ K are presented in Figure 6 (see Figure S3 in the Supporting Information for complete data). The ^{1}H NMR spectroscopic peaks in Figure 6 (left) were integrated and normalized to deduce the mole fraction for each species (Figure 6, right). Individual kinetic rate constants could then be obtained by fitting the mole fractions with the Berkeley Madonna Software[23] and considering **Cc** as an intermediate species between **B** and **Ct** (Scheme 4).

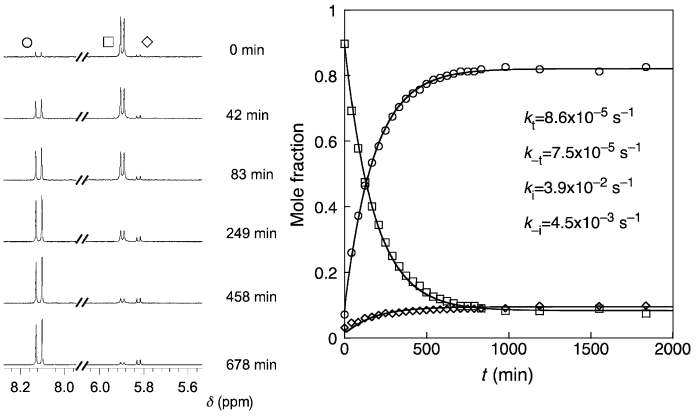

Figure 6. Left) Kinetics of the thermal recovery at 308 K of irradiated solutions of compound **1** at neutral pD in CD_3OD/D_2O 1:1, followed by 600 MHz ^{1}H NMR spectroscopy: **Ct** H4 (○); **B** H3 (□); **Cc** H3 (◇). Right) The data was fitted by loading Equations (11), (12), and (13) into Berkeley Madonna Software,[23] imposing the constraints $K_t = k_t/k_{-t}$ and $K_i = k_i/k_{-i}$, and using the values from the plateaus to calculate K_t and K_i.

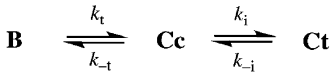

Scheme 4. Kinetic scheme for the thermal recovery of irradiated solutions of **1** in neutral media.

On the basis of the kinetics in Scheme 4, Equations (11), (12), and (13) were used in the fitting:

$$\frac{d[\mathbf{B}]}{dt} = -k_t[\mathbf{B}] + k_{-t}[\mathbf{Cc}] \quad (11)$$

$$\frac{d[\mathbf{Cc}]}{dt} = -(k_{-t} + k_i)[\mathbf{Cc}] + k_t[\mathbf{B}] + k_{-i}[\mathbf{Ct}] \quad (12)$$

$$\frac{d[\mathbf{Ct}]}{dt} = -k_{-i}[\mathbf{Ct}] + k_t[\mathbf{Ct}] \quad (13)$$

The kinetics in Figure 6 (right) are nicely fitted with the equations derived from Scheme 4, thus showing the existence of an intermediate assigned to **Cc** (see the NMR spectroscopic data below). Also the plateaus observed upon equilibration yield constants ($K_t = 1.1$, $K_i = 8.6$, 308 K) that are in relatively good agreement with the ones obtained from thermal evolution starting from **Ct** ($K_t = 1.0$, $K_i = 8.0$, 300 K). The mechanism of formation of **Ct** from **B** in Scheme 4 is in accordance with the one usually observed for several related 2-hydroxychalcones.[8] However, in 2-hydroxychalcones, the **Cc** is often an elusive compound; it exists in fast equilibrium with the hemiketal **B**, with rate constants on the sub-second timescale. Figure 6 (right) clearly shows that in compound **1**, **B** and **Cc** equilibrate on a much longer timescale, approximately four orders of magnitude slower. To explain this difference in the tautomerization rates between **Cc** and **B** derived from 2-phenyl- and from 2-(4′-pyridine)-1-benzopyrylium, the formal charges were calculated (AM1-RHF level, Figure S4 and Table S4 in the Supporting Information). The **Cc** derived from **1** shows a charge density at the phenolic oxygen considerably lower than the charge at the same atom in the parent compound (−0.250 vs. −0.364). This lower charge reflects the lower nucleophilicity of the oxygen. At the same time, the **Cc** derived from compound **1** shows a slightly lower positive charge (lower electrophilicity) at the carbonyl carbon where the nucleophilic ring-closure reaction occurs (+0.319 vs. +0.342). Thus, a slower ring closure is expected for the **Cc** derived from compound **1**, as experimentally observed.

In the case of **B** derived from compound **1**, in which the σ bond is already formed and has to be broken to lead to **Cc**, the charge densities (at the same oxygen and carbon atoms) reflect the ionic contribution for the bond energy or the recombination efficiency after bond breaking (aborting **Cc** formation). In this case, the charge densities at O9 and C2 are larger in the case of **B** derived from compound **1**, which is expected to lower the efficiency of **Cc** formation as experimentally observed.

It is known that the hemiketal/*cis*-chalcone tautomerization equilibrium in flavylium derivatives is catalyzed by acids.[7,13] The addition of a drop of concentrated acid to an irradiated solution of **Ct** containing approximately 100% **B** shows the immediate formation of protonated $\mathbf{Cc}^+$ and $\mathbf{B}^+$ species, thereby underlining a huge difference between the kinetic rate constants for tautomerization under acidic and

neutral conditions (Figure S5 in the Supporting Information).

The kinetic constants obtained for the direct and reverse tautomerization and *cis–trans* isomerization reactions at different temperatures were plotted using the Eyring equation (Figure 7) to deduce the respective thermodynamic activation parameters ($\Delta H^{\neq}$, $\Delta S^{\neq}$, and $\Delta G^{\neq}$; Table 1).

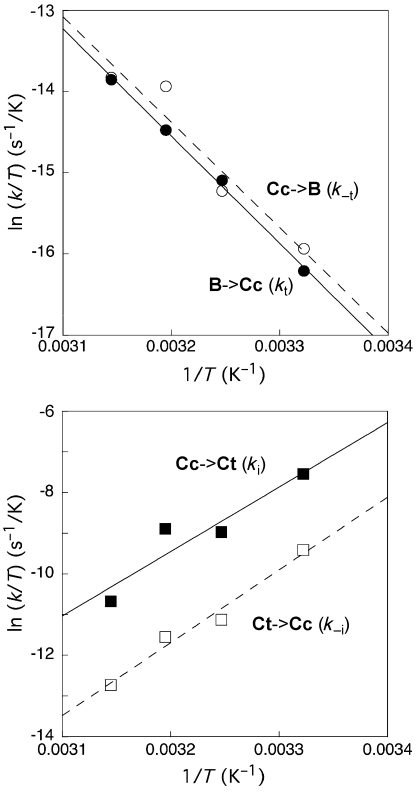

Figure 7. Eyring plots for the direct (k_t, ●, ——) and reverse (k_{-t}, ○, – – –) tautomerization (top) and for *cis–trans* (k_i, ■, ——) and *trans–cis* (k_{-i}, □, – – –) isomerization reactions of **1** (bottom).

Table 1. Thermodynamic activation parameters for the direct and reverse tautomerization and isomerization reactions of **1**.

	B→Cc	**Cc→B**	**Cc→Ct**	**Ct→Cc**
$\Delta H^{\neq}$ [kJ mol^{-1}]	109.9	108.0	−131.8	−148.8
$\Delta S^{\neq}$ [J K^{-1} mol^{-1}]	35.2	30.7	−695.6	−768.7
$\Delta G^{\neq}$ [kJ mol^{-1}] (300 K)	99.3	98.8	76.9	81.8

The similarity of the free energies of activation, $\Delta G^{\neq}$, for the ring-opening (**B→Cc**) and for the ring-closure (**Cc→B**) processes reflect the same order of magnitude of the k_t and k_{-t} rate constants, respectively 8.6×10^{-5} and 7.5×10^{-5} s^{-1} (308 K). On the other hand, the lower value of $\Delta G^{\neq}$ for the *cis–trans* relative to the *trans–cis* isomerization reflects the relation $k_i = 3.9\times10^{-2}$ s^{-1} > $k_{-i} = 4.5\times10^{-3}$ s^{-1} (308 K). The equilibrium constants at 300 K calculated from $\Delta G^{\circ}_t = \Delta G^{\neq}$(**B→Cc**)$-\Delta G^{\neq}$(**Cc→B**) and $\Delta G^{\circ}_i = \Delta G^{\neq}$(**Cc→Ct**)$-\Delta G^{\neq}$(**Ct→Cc**) yield $K_t = 0.8$ and $K_i = 7.2$, which are in relatively good agreement with the data in Scheme 3. In the tautomerization reaction, the ring-opening and the ring-closure processes are characterized by low activation entropies ($\Delta S^{\neq}$). In spite of the fact that **B** has a closed structure and **Cc** an open one, the most stable conformation of **Cc** is not expected to differ much from the structure of **B**; **Cc** is almost preorganized for ring closure. A search for lowest energy conformers (see above) yields a structure for **Cc** showing an intramolecular hydrogen bond between the carbonyl group and the phenolic hydrogen, a structure even more similar to that of **B**, thereby corroborating the similarity of the experimentally observed values for $\Delta S^{\neq}$ for **B→Cc** and **Cc→B**.

Regarding the isomerization reaction, strongly negative activation entropies are observed for both processes, thereby indicating a transition state with a more constrained structure than those of **Cc** and **Ct**. More striking is the fact that negative activation enthalpies ($\Delta H^{\neq}$) are also observed for both processes. Negative temperature effects on reaction rates have been rationalized by the postulate of an intermediate in a pre-equilibrium situation or in elementary reactions when very negative activation entropies are observed.[24] In the present case, both situations can be evoked: in the former hypothesis, a tautomer formed from **Cc** or **Ct** could be involved as an intermediate, and similar 2-hydroxychalcones are known to have tautomers;[25] the latter hypothesis applies directly in the face of the strongly negative activation entropies observed.

The overall thermodynamic and kinetic data obtained for compound **1** are summarized in Scheme 5.

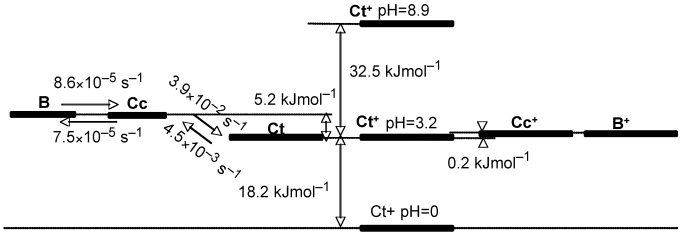

Scheme 5. Thermodynamic diagram and kinetic constants for the reaction network of compound **1** in acidic and neutral conditions.

Photochemistry: Irradiation of compound **1** (MeOH/H_2O 1:1, pH 6.0) was carried out at 365 nm, near the λ_{max} of **Ct** (Figure 8A). The spectral variations are compatible with the disappearance of **Ct** and concomitant formation of **B** or **Cc**, or both, with a quantum yield (Φ) of 0.02. Irradiation at 254 nm of the previous photostationary state (obtained upon irradiation at 365 nm) leads to the recovery of **Ct** up to around 80% with a quantum yield of $\Phi = 0.21$ (Figure 8B). Under acidic conditions (MeOH/H_2O 1:1, pH 1.0), in which equilibrated solutions of compound **1** contain approximately one third of each protonated species (**Ct⁺**, **Cc⁺**, and **B⁺**), irradiation at 254 nm gives rise to spectral modifications showing that **Ct⁺** is formed from **B⁺** and/or **Cc⁺** (Figure 8C).

On the other hand, in pure aqueous solution at pH 1.0, where only **Ct⁺** (45%) and **B⁺** (55%) are present, the for-

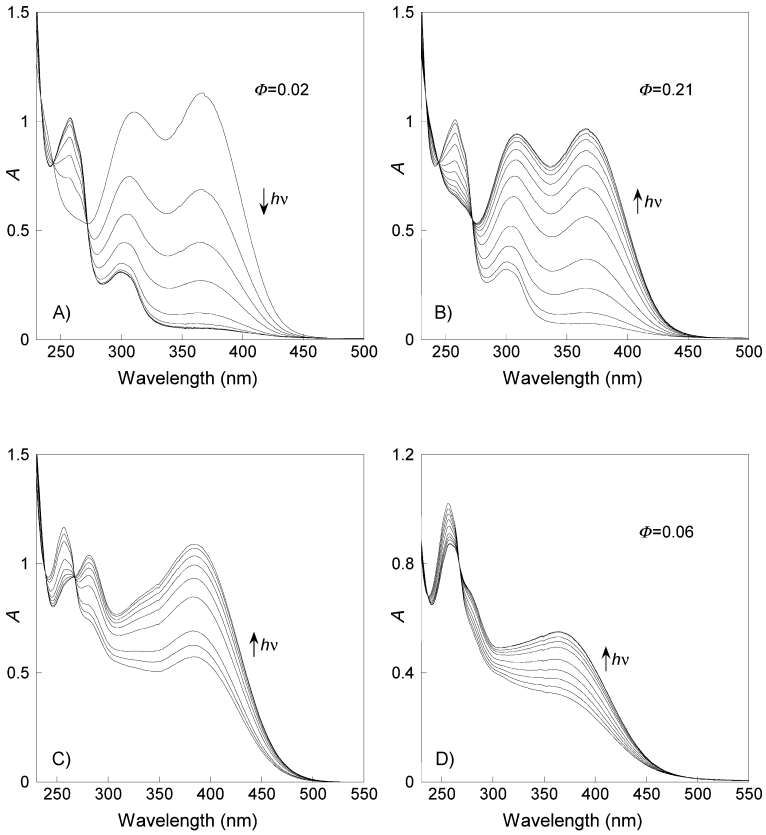

Figure 8. Continuous irradiation of compound **1** (1.0×10^{-4} M in MeOH/H_2O 1:1). A) Irradiation of a fresh solution at pH 6.0 (100% **Ct**), $\lambda_{irr}=365$ nm. B) Irradiation of the solution obtained in A at $\lambda_{irr}=254$ nm. C) Irradiation of an equilibrated solution at pH 1.0 (37% $\mathbf{Ct^+}$, 31.5% $\mathbf{Cc^+}$, 31.5% $\mathbf{B^+}$), $\lambda_{irr}=254$ nm. D) Irradiation of an equilibrated aqueous solution of **1** at pH 1.0 (45% $\mathbf{Ct^+}$, 55% $\mathbf{B^+}$), $\lambda_{irr}=254$ nm in water.

mation of $\mathbf{Ct^+}$ upon irradiation of $\mathbf{B^+}$ at 254 nm gives a direct evidence of the photochromism of the protonated chromene (Figure 8D). The presence of an isosbestic point ($\lambda=260$ nm) shows that $\mathbf{Cc^+}$ does not appear during irradiation. In the basic region, no significant spectral variations were observed upon one hour of irradiation at 365 nm, thereby showing that the $\mathbf{Ct^-}$ species is photochemically inactive.

To characterize the species that are formed upon irradiation of neutral solutions of **1** (CD_3OD/D_2O 1:1) at 365 nm, ^{1}H NMR spectra were run before, during, and after reaching the photostationary state (traces a, b, and c in Figure 9, respectively). The *trans*-chalcone **Ct** was converted in one unique product characterized by a lower coupling constant between protons H3 and H4 (^3J(H3,H4) = 9.8 vs. 16.0 Hz for **Ct**). No other species were observed during the irradiation, or at the photostationary state. The rather close ^{1}H chemical shifts of **Cc** and **B** (e.g., $\delta=5.83$ vs. 5.88 ppm for H3; Table S1 in the Supporting Information) do not allow one to conclude which of them is the observed photochemical product. However, the ^{13}C chemical shift of the carbonyl found in **Cc** and that of the carbon in the hemiketal group of **B** are expected to be quite different.[26] Heteronuclear multiple-bond correlation (HMBC) spectra registered after reaching the photostationary state are presented in Figure 10 (for full ^{13}C assignments, see Tables S5 and S6 in the Supporting Information). Two sets of resonances are present and are attributed to the photoproduct and to some (thermal) recovery of **Ct** during the time of the experiment. Strong differences between the two products can be observed. In particular, the large difference in chemical shifts in carbon atoms C2 ($\delta=$ 192.8 ppm in **Ct** vs. 95.7 ppm in the photoproduct) and C4 ($\delta=$ 141.1 vs. 125.3 ppm) are not compatible with the presence of a carbonyl group in the photoproduct, thus proving that it must be assigned to the hemiketal **B** and that no **Cc** is formed. Exclusive formation of a hemiketal upon irradiation of some *trans*-2-hydroxychalcones was claimed by Hiratsuka et al. on the basis of UV/Vis absorption and ^{1}H NMR spectra, but no conclusive ^{13}C NMR spectroscopic data was presented.[17] The lack of **Cc** upon irradiation of **Ct** can only be explained if an efficient photochemical step converts **Cc** into **B** (photo ring closure), since the thermal conversion of **Cc** into **B** is very slow when the phenyl ring is substituted by pyridine, as seen above.

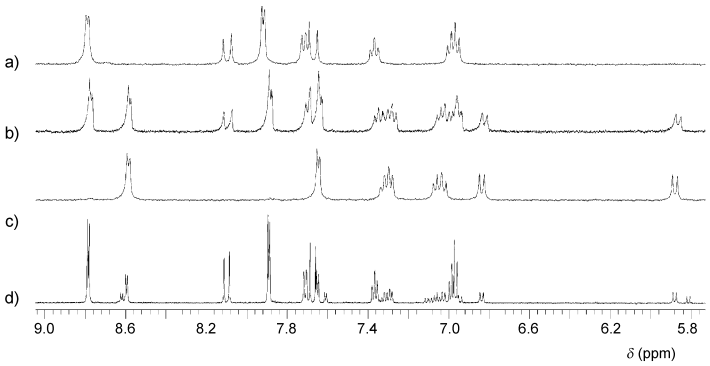

Figure 9. ^{1}H NMR spectra (400 MHz, a–c; 600 MHz, d; 300 K) of **1** in D_2O/CD_3OD 1:1 at a) neutral solution, pD ≈ 6.0, before irradiation (100% **Ct**); b) in the course of irradiating at 365 nm; c) after reaching the photostationary state upon irradiation at 365 nm (≈100% **B**); d) after thermal equilibration of the irradiated solution in (c).

The thermal recovery of the irradiated solution (ca. 100% **B**; Figure 9c) was followed by ^{1}H NMR spectroscopy with

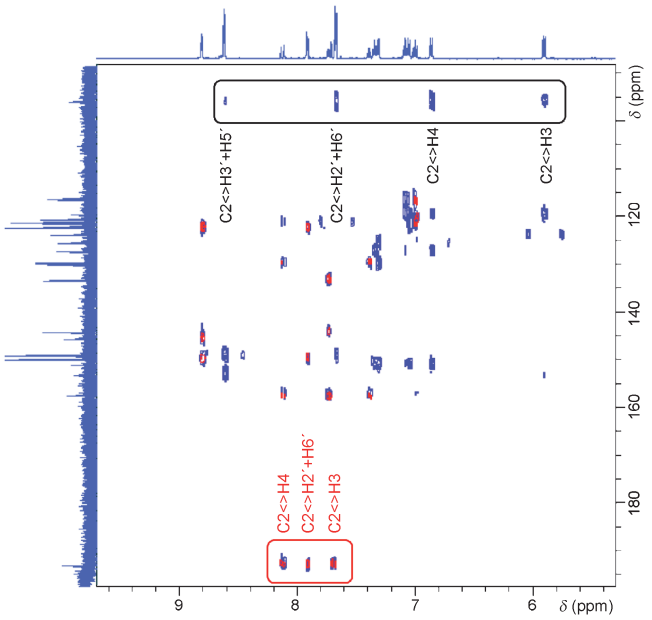

Figure 10. HMBC spectra (600 MHz, 300 K) of **1** in D_2O/CD_3OD 1:1, pD ≈6 before (red) and after irradiation at 365 nm (blue). In the black box are the correlations between C2 and H3′+H5′, H2′+H6′, H4, and H3 in **B**; in the red box are the correlations between C2 and H4, H2′+H6′, and H3 in **Ct**.

formation of **B** and **Cc** in equilibrium with **Ct**, as reported above in Figures 6 and 9d.

The photochemical product of the irradiation of **Ct** at 365 nm, approximately 100% **B** ($MeOH/H_2O$ 1:1), was irradiated at 254 nm, a wavelength at which this last species absorbs. The photostationary state thus obtained (Figure 8B) is composed of approximately 80% **Ct** and 20% **B**. This result is compatible with a photo ring opening of **B** to give the *cis*-enol that could give **Ct**, since enolization is known to be very fast in the presence of protic solvents, followed by *cis*–*trans* photoisomerization to form **Ct**.[17] Alternatively, the *cis*-enol could tautomerize to **Cc** and this one photoisomerize to **Ct**, as observed in some *cis*-2-hydroxychalcones (Scheme 6).[27]

In both photochemical reactions of Figure 8A and B, the **Cc** was not detected by ^1H NMR spectroscopy or spectrophotometry. In the first case, by the reason reported above (fast enolization), and in the second one by an efficient **Cc** to **Ct** photoisomerization. A similar behavior was reported for 4′-methoxyflavylium for which $\Phi_{Ct-Cc}=0.04$ and $\Phi_{Cc-Ct}=0.5$.[27b]

In acidic media ($MeOH/H_2O$ 1:1), the irradiation of an equilibrated mixture of compound **1** ($\lambda_{irr}=254$ nm, pH 1.0, 37% $\mathbf{Ct^+}$, 31.5% $\mathbf{Cc^+}$, 31.5% $\mathbf{B^+}$) produces a photostationary state in which $\mathbf{Ct^+}$ is the predominant species, a result qualitatively similar to the one obtained at neutral pH values (Figure 8C). In water, at pH 1.0, a similar situation was observed (Figure 8D).

Conclusion

The insertion of a pyridine group in the 2-hydroxychalcone structure considerably modifies the chemical reaction network, excluding the formation of the flavylium ion and showing $\mathbf{B^+}$ and $\mathbf{Cc^+}$ as the stable species in very acid media. All the species of the network have been characterized by ^1H NMR spectroscopy (most by ^{13}C NMR spectroscopy as well) and steady-state absorption. In particular, the hemiketal **B** (a hydroxy-4-pyridinechromene) and the *cis*-chalcone **Cc** were clearly characterized by ^{13}C NMR spectroscopy. The ring opening/closure is unusually slow when compared with the same process in 2-hydroxychalcone derivatives, which was explained in terms of different electronic charge densities. In an acid medium, the ring-opening/closure tautomerization process is much faster and similar to the one observed for 2-hydroxychalcones derivatives due to acid catalysis.

The irradiation of **Ct** produces **B** through two consecutive photochemical reactions: **Ct**→**Cc** photoisomerization followed by **Cc**→**B** photo ring closure with a global quantum yield of 0.02. On the other hand, irradiation of **B** leads to a photostationary state composed of 80% **Ct** and 20% **B**, with a quantum yield of 0.21.

Experimental Section

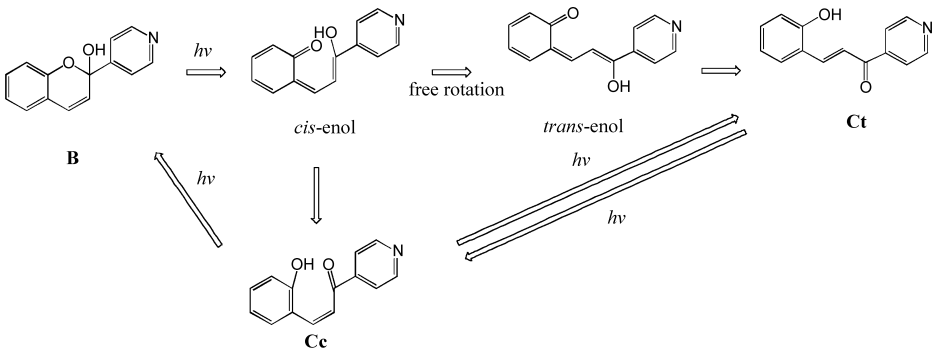

Scheme 6. General scheme for a dual photochromic system involving chromene(hemiketal), *cis*-chalcone, and *trans*-chalcone.

Synthesis: All reagents and solvents used were of analytical grade. The NMR spectra at 298.0 K were obtained using a Bruker AMX400 operating at 400.13 (^1H) and 100 MHz (^{13}C) or on a Bruker Avance 600 operating at 600.13 Hz (^1H) and 150.91 Hz (^{13}C). Mass spectra experiments were run using an Applied Biosystems Voyager PRO (MALDI-TOF MS). Elemental analyses was performed using a Thermofinnigan Flash EA 1112 Series instrument.

Synthesis of compound 1: A degassed solution of potassium hydroxide (1.0 g, 17.8 mmol) dissolved in a minimum amount of water was added under an argon atmosphere at room tempera-

ture to a stirred, degassed solution of 4-acetylpyridine (1.21 g, 10 mmol) and salicylaldehyde (1.22 g, 10 mmol) in ethanol. The solution turned red instantaneously, thereby indicating the deprotonation of the phenol group. The reaction mixture was stirred at room temperature overnight. After this period, the solution was neutralized and concentrated under reduced pressure. The resulting solid was filtered and purified by column chromatography on silica gel using a mixture of dichloromethane/ethyl acetate (80:20, v/v). The solvent was evaporated to yield a yellow solid (510 mg, 23%). ^{1}H NMR (400 MHz, CD_3OD/D_2O 1:1, 25°C): $\delta = 8.79$ (d, J(H2′–H6′,H3′–H5′) = 5.4 Hz, 2H; H3′–H5′), 8.09 (d, J(H3,H4) = 16.0 Hz, 1H; H4), 7.92 (d, J(H2′–H6′,H3′–H5′) = 5.4 Hz, 2H; H2′–H6′), 7.66 (d, J-(H3,H4) = 16.0 Hz, 1H; H3), 7.71 (d, J(H5,H6) = 7.5 Hz, 1H; H5), 7.37 (t, J(H7,H8) = 8.1 Hz, J(H6,H7) = 7.1 Hz, 1H; H7), 6.99 (t, J(H5,H6) = 7.5 Hz, J(H6,H7) = 7.1 Hz, 1H; H6), 6.96 ppm (d, J(H7,H8) = 8.1 Hz, 1H; H8); ^{13}C NMR (100 MHz, CD_3OD/D_2O 1:1, 25°C): $\delta = 192.8$ (C9), 157.2 (C2), 150.2 (C3–C5′), 145.4 (C1′), 144.1 (C4), 133.2 (C7), 129.5 (C5), 122.2 (C2′–C6′), 121.2 (C3), 121.1 (C10), 120.5 (C6), 116.3 ppm (C8); MS (MALDI-TOF): m/z: 225.1 [M^+]; elemental analysis calcd (%) for $C_{14}H_{11}NO_2$: C 74.65, N 6.22, H 4.92; found: C 74.57, N 6.35, H 5.08.

Measurements: Solutions were prepared using Millipore water and spectroscopic methanol (when needed). The solution pH was adjusted by addition of HCl, NaOH, or the universal buffer of Theorell and Stenhagen,[28] and was measured using a Radiometer Copenhagen PHM240 pH/ion meter. UV/Vis absorption spectra were recorded using a Varian-Cary 100 Bio spectrophotometer or on a Shimadzu VC2501-PC. For NMR spectroscopy experiments, compound **1** was dissolved in a solution of D_2O and CD_3OD. When required, the pH was adjusted by addition of small aliquots of DCl (ca. 0.5 M) or NaOD (0.1 M). Photoexcitation in continuous irradiation experiments were carried out using a xenon/medium-pressure mercury arc lamp, and the excitation bands (254 and 365 nm) were isolated with interference filters (Oriel). The incident light intensity was measured by ferrioxalate actinometry.[29]

Acknowledgements

We acknowledge LabRMN at FCT-UNL and Rede Nacional de RMN (supported with funds from FCT-MCTES) for access to the facilities. The Portuguese FCT-MCTES is also acknowledged for financial support through project PTDC/QUI/67786/2006 and a post-doc grant SFRH/BPD/44230/2008 (Y.L.). J. C. Lima, C. Laia, and V. Petrov are kindly acknowledged for fruitful discussions.

[1] a) E. E. Schweizer, O. Meeder-Nycz in *Chromenes, Chromanes, Chromones* (Ed.: G. P. Ellis), Wiley-Interscience, New York, **1977**; b) A. F. Benslimane, Y. F. Pouchus, J.-F. Verbist, J.-Y. Petit, J. D. Brion, L. Welin, *J. Clin. Pharmacol.* **1995**, *35*, 298–301; c) K. C. Nicolaou, J. A. Pfefferkorn, A. J. Roecker, G. Q. Cao, S. Barluenga, H. J. Mitchell, *J. Am. Chem. Soc.* **2000**, *122*, 9939–9953; d) V. Rukachaisirikul, M. Kamkaew, D. Sukavisit, S. Phongpaichit, P. Sawangchote, W. C. Taylor, *J. Nat. Prod.* **2003**, *66*, 1531–1535.

[2] a) H. Bouas-Laurent, H. Dürr, *Pure Appl. Chem.* **2001**, *73*, 639–665; b) H. Dürr in *Photochromism: Molecules and Systems* (Eds.: H. Dürr, H. Bouas-Laurent), Elsevier, Amsterdam, **2003**; c) *Organic Photochromic and Thermochromic Compounds* (Eds.: J. C. Crano, R. J. Guglielmetti), Plenum Press, New York, **1999**.

[3] a) R. S. Becker, J. Michl, *J. Am. Chem. Soc.* **1966**, *88*, 5931–5933; b) J. Kolc, R. S. Becker, *J.Phys. Chem.* **1967**, *71*, 4045–4048; c) R. S. Becker, J. Kolc, *J. Phys. Chem.* **1968**, *72*, 997; d) R. S. Becker, E. Dolan, D. E. Balke, *J. Chem. Phys.* **1969**, *50*, 239–245; e) N. W. Tyer, R. S. Becker, *J. Am. Chem. Soc.* **1970**, *92*, 1289–1294; f) N. W. Tyer, R. S. Becker, *J. Am. Chem. Soc.* **1970**, *92*, 1295–1302; g) J. Kolc, R. S. Becker, *Photochem. Photobiol.* **1970**, *12*, 383–393; h) L. Edwards, J. Kolc, R. S. Becker, *Photochem. Photobiol.* **1971**, *13*, 423–429; i) J. Kolc, R. S. Becker, *J. Chem. Soc. Perkin Trans. 2* **1972**, 17; j) C. Lenoble, R. S. Becker, *J. Photochem.* **1986**, *33*, 187–197.

[4] *Molecular Switches* (Ed.: B. L. Feringa), Wiley-VCH, Weinheim, **2001**.

[5] a) T. Swain in *The Flavonoids* (Eds.: J. B. Harborne, T. J. Mabry, H. Mabry), Chapman and Hall/CRC Press, London, **1975**, pp. 1096–1129; b) *Anthocyanins as Food Colors* (Ed.: P. Markakis), Academic Press, New York, **1982**; c) R. Brouillard, O. Dangles in *The Flavonoids: Advances in Research Since 1986* (Ed.: J. B. Harborne), Chapman and Hall/CRC Press, New York, pp. 565–588.

[6] a) R. Brouillard, J.-E. Dubois, *J. Am. Chem. Soc.* **1977**, *99*, 1359–1364; b) R. Brouillard, B. Delaporte, *J. Am. Chem. Soc.* **1977**, *99*, 8461–8468; c) R. Brouillard, B. Delaporte, J.-E. Dubois, *J. Am. Chem. Soc.* **1978**, *100*, 6202–6205.

[7] a) R. A. McClelland, S. Gedge, *J. Am. Chem. Soc.* **1980**, *102*, 5838–5848; b) R. A. McClelland, G. H. McGall, *J. Org. Chem.* **1982**, *47*, 3730–3736; c) D. B. Devine, R. A. McClelland, *J. Org. Chem.* **1985**, *50*, 5656–5660.

[8] a) F. Pina, M. Maestri, V. Balzani, *Chem. Commun.* **1999**, 107–114; b) M. Maestri, F. Pina, V. Balzani, in *Molecular Switches* (Ed.: L. B.Feringa), Wiley-VCH, Weinheim, **2001**, pp. 309–334; c) F. Pina, M. Maestri, V. Balzani in *Handbook of Photochemistry and Photobiology, Vol. 3* (Ed.: H. S. Nalwa), American Science Publishers, Los Angeles, **2003**, pp. 411–449.

[9] a) A. Roque, C. Lodeiro, F. Pina, M. Maestri, S. Dumas, P. Passaniti, V. Balzani, *J. Am. Chem. Soc.* **2003**, *125*, 987–994; b) M. C. Moncada, D. Fernández, J. C. Lima, A. J. Parola, C. Lodeiro, F. Folgosa, M. J. Melo, F. Pina, *Org. Biomol. Chem.* **2004**, *2*, 2802–2808; c) L. Giestas, F. Folgosa, J. C. Lima, A. J. Parola, F. Pina, *Eur. J. Org. Chem.* **2005**, 4187–4200; d) C. A. T. Laia, A. J. Parola, F. Folgosa, F. Pina, *Org. Biomol. Chem.* **2007**, *5*, 69–77.

[10] A. Roque, C. Lodeiro, F. Pina, M. Maestri, R. Ballardini V. Balzani, *Eur. J. Org. Chem.* **2002**, 2669–2709.

[11] a) H. Santos, D. L. Turner, J. C. Lima, P. Figueiredo, F. Pina, A. L. Maçanita, *Phytochemistry* **1993**, *32*, 1227–1232; b) F. Pina, *J. Chem. Soc. Faraday Trans.* **1998**, *94*, 2109–2116.

[12] a) F. Pina, M. J. Melo, S. Alves, R. Ballardini, M. Maestri, P. Passaniti, *New J. Chem.* **2001**, *25*, 747–752; b) M. C. Moncada, S. Moura, M. J. Melo, A. Roque, C. Lodeiro, F. Pina, *Inorg. Chim. Acta* **2003**, *356*, 51–61.

[13] a) V. Petrov, R. Gomes, A. J. Parola, F. Pina, *Dyes Pigm.* **2009**, *80*, 149–155; b) F. Pina, M. J. Melo, M. Maestri, P. Passaniti, V. Balzani, *J. Am. Chem. Soc.* **2000**, *122*, 4496–4498.

[14] a) R. Matsushima, K. Miyakawa, M. Nishihata, *Chem. Lett.* **1988**, 1915–1916; b) R. Matsushima, M. Suzuki, *Bull. Chem. Soc. Jpn.* **1992**, *65*, 39–45; c) R. Matsushima, H. Mizuno, A. Kajiura, *Bull. Chem. Soc. Jpn.* **1994**, *67*, 1762–1764; d) R. Matsushima, H. Mizuno, H. Itoh, *J. Photochem. Photobiol. A* **1995**, *89*, 251–256; e) R. Matsushima, T. Murakami, *Bull. Chem. Soc. Jpn.* **2000**, *73*, 2215–2219; f) R. Matsushima, S. Fujimoto, K. Tokumura, *Bull. Chem. Soc. Jpn.* **2001**, *74*, 827–832; g) K. Tokumura, N. Taniguchi, T. Kimura, R. Matsushima, *Chem. Lett.* **2001**, 126–127; h) R. Matsushima, K. Kato, S. Ishigai, *Bull. Chem. Soc. Jpn.* **2002**, *75*, 2079–2080.

[15] a) H. Wunscher, G. Haucke, P. Czerney, U. Kurzer, *J. Photochem. Photobiol. A* **2002**, *151*, 75–82; b) H. Wünscher, G. Haucke, P. Czerney, *J. Photochem. Photobiol. A* **2002**, *152*, 61–71.

[16] a) Y. Norikane, H. Itoh, T. Arai, *J. Phys. Chem. A* **2002**, *106*, 2766-2776; b) K. Kaneda, T. Arai, *Org. Biomol. Chem.* **2003**, *1*, 2041–2043.

[17] a) H. Horiuchi, A. Yokawa, T. Okutsu, H. Hiratsuka, *Bull. Chem. Soc. Jpn.* **1999**, *72*, 2429–2435; b) H. Horiuchi, H. Shirase, T. Okutsu, R. Matsushima, H. Hiratsuka, *Chem. Lett.* **2000**, 96–97; c) H. Horiuchi, A. Tsukamoto, T. Okajima, H. Shirase, T. Okutsu, R. Matsushima, H. Hiratsuka, *J. Photochem. Photobiol. A* **2009**, *205*, 203–209.

[18] A. E. Martell, R. M. Smith, R. M. Moteikaitis, *NIST Critical Stability Constants Database*, Texas A&M, University College Station, **1993**.

[19] a) M. C. Moncada, F. Pina, A. Roque, A. J. Parola, M. Maestri, V. Balzani, *Eur. J. Org. Chem.* **2004**, 304–312; b) D. Fernández, F. Folgosa, A. J. Parola, F. Pina, *New J. Chem.* **2004**, *28*, 1221–1226.

[20] R. Gomes, A. J. Parola, C. A. T. Laia, F. Pina, *J. Phys. Chem. B* **2007**, *111*, 12059–12065.

[21] R. Gomes, A. J. Parola, C. A. T. Laia, F. Pina, *Photochem. Photobiol. Sci.* **2007**, *6*, 1003–1009.

[22] A. Roque, J. C. Lima, A. J. Parola, F. Pina, *Photochem. Photobiol. Sci.* **2007**, *6*, 381–385.

[23] Berkeley Madonna X (Mach-O), Version 8.3.18, developed by Robert Macey, George Oster, University of California, Berkeley, **2006**.

[24] a) R. Frank, G. Greiner, H. Rau, *Phys. Chem. Chem. Phys.* **1999**, *1*, 3481–3490; b) E. I. Kapinus, H. Rau, *J. Phys. Chem. A* **1998**, *102*, 5569–5576.

[25] a) A. M. Diniz, R. Gomes, A. J. Parola, C. A. T. Laia, F. Pina, *J. Phys. Chem. B* **2009**, *113*, 719—727; b) A. Roque, J. C. Lima, A. J. Parola, F. Pina, *Photochem. Photobiol. Sci.* **2007**, *6*, 381–385.

[26] *Carbon-13 NMR of Flavonoids* (Ed.: P. K. Agrawal), Elsevier, Amsterdam, **1989**.

[27] a) A. Jimenez, C. Pinheiro, A. J. Parola, M. Maestri, F. Pina, *Photochem. Photobiol. Sci.* **2007**, *6*, 372–380; b) F. Pina, M. J. Melo, M. Maestri, R. Ballardini, V. Balzani, *J. Am. Chem. Soc.* **1997**, *119*, 5556–5561.

[28] F. W. Küster, A. Thiel, *Tabelle per le Analisi Chimiche e Chmico-Fisiche*, 12th ed., Hoepli, Milano, **1982**, pp. 157–160. The universal buffer used was prepared in the following way: 85% (w/w) phosphoric acid (2.3 cm^3), monohydrated citric acid (7.00 g), and boric acid (3.54 g) were dissolved in water; 1 M NaOH (343 mL) was then added, and the solution was diluted to 1 dm^3 with water.

[29] C. G. Hatchard, C. A. Parker, *Proc. R. Soc. London Ser. A* **1956**, *235*, 518–536.

[30] Hyperchem, release 6.01 for windows, Copyright Hypercube, Inc., Gainesville, **2000**.

Received: July 7, 2009
Published online: November 13, 2009

